

SUPPLEMENTARY INFORMATION

Mucus production, host-microbiome interactions, hormone sensitivity, and innate immune responses modeled in human cervix chips

Zohreh Izadifar¹, Justin Cotton¹, Siyu Chen², Viktor Horvath¹, Anna Stejskalova¹, Aakanksha Gulati¹, Nina T. LoGrande¹, Bogdan Budnik¹, Sanjid Shahriar¹, Erin R. Doherty¹, Yixuan Xie², Tania To¹, Sarah E. Gilpin¹, Adama M. Sesay¹, Girija Goyal¹, Carlito Lebrilla², and Donald E. Ingber^{1,3,4*}

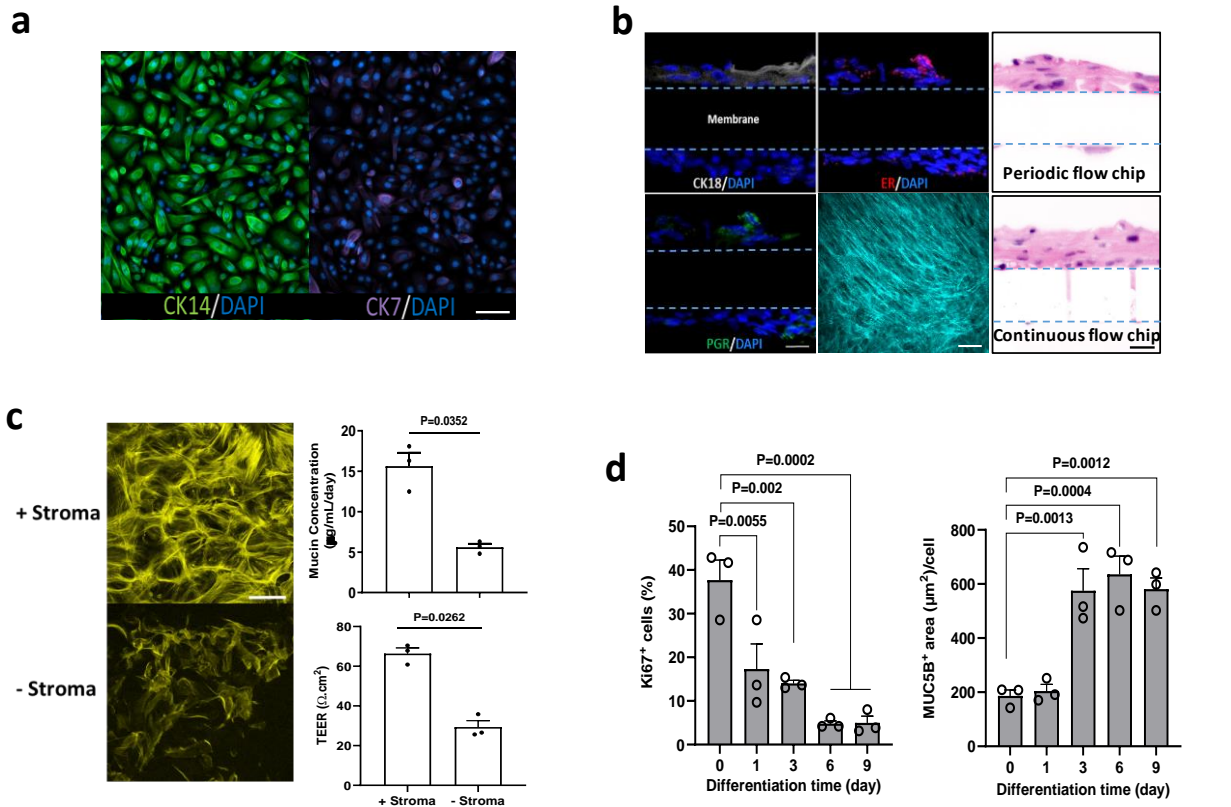
¹Wyss Institute for Biologically Inspired Engineering, Harvard University, Boston, MA 02215

²Department of Chemistry, University of California Davis, Davis, California, CA 95616

³Vascular Biology Program, Boston Children's Hospital and Department of Pathology, Harvard Medical School, Boston, MA 02115

⁴Harvard John A. Paulson School of Engineering and Applied Sciences, Cambridge, MA 02134

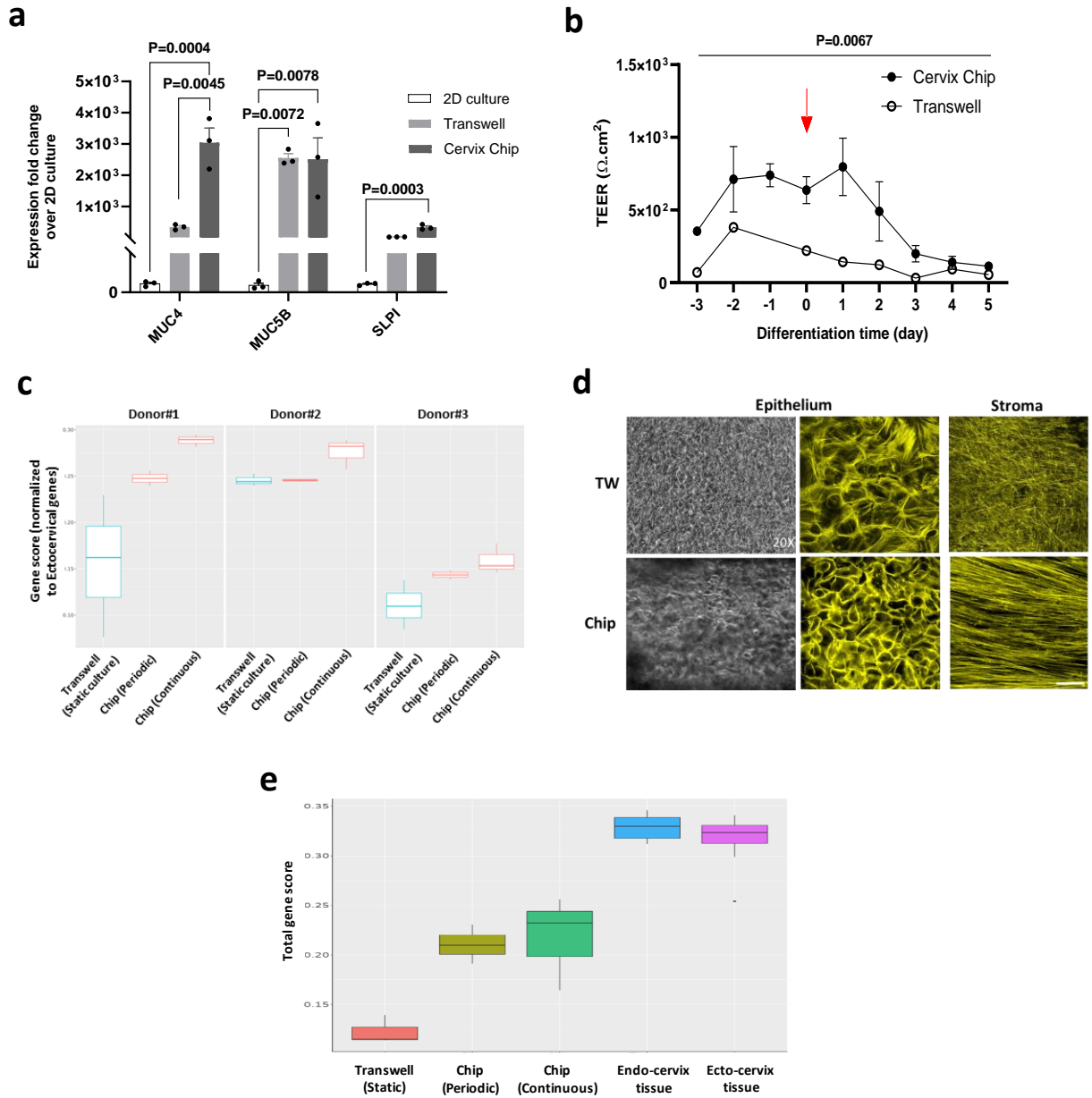
*Address all correspondence to: don.ingber@wyss.harvard.edu



Supplementary Fig. S1. Characterization of the human Cervix Chip. a. Immunofluorescence

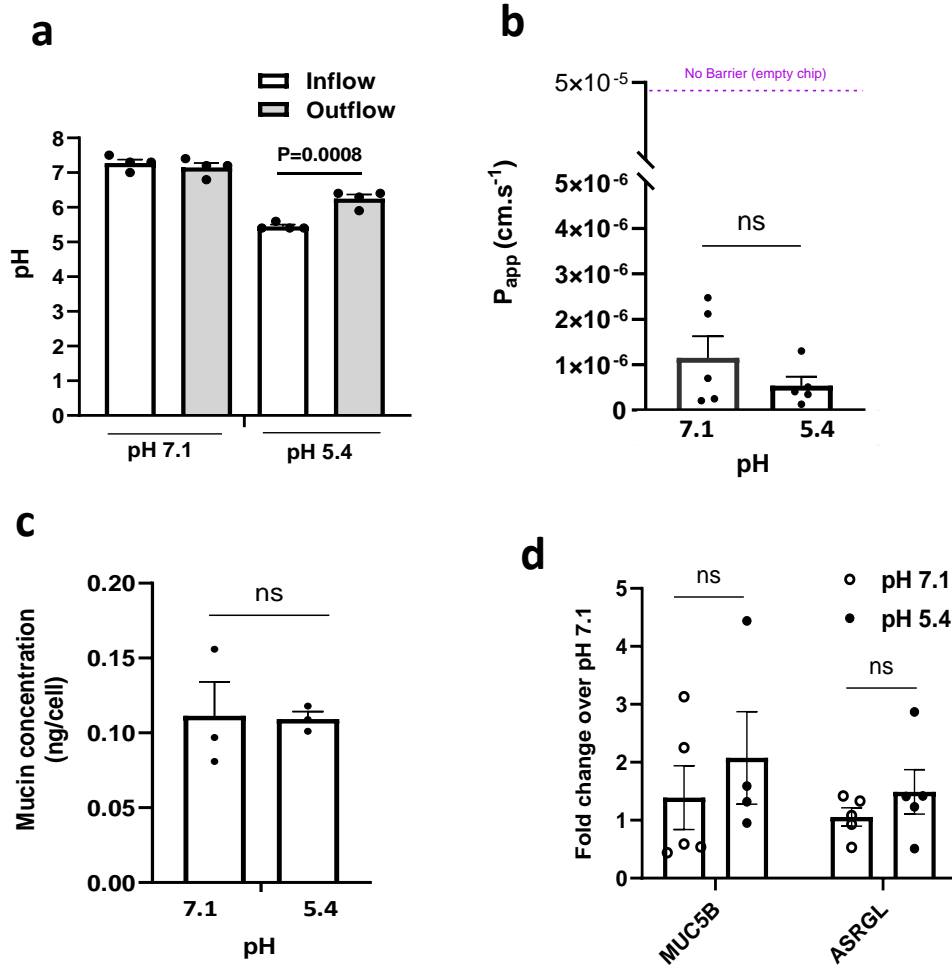
micrographs of the cervical epithelial cells in 2D culture stained for cytokeratin 14 (CK14, green) (left) and cytokeratin 7 (CK7, magenta) (right) showing a mixture of primary human endo- and ecto-cervical epithelial cells, respectively (bar, 100 µm). **b.** Immunofluorescence microscopic vertical cross sectional views of the chip showing the cervical epithelium stained at day 7 of differentiation for cytokeratin 18 (CK18, white) (top left), estrogen receptor (ER, red) (middle top), progesterone receptor (PR, green) (bottom left), and Hoechst-stained nuclei (blue) (bar, 20 µm), and second harmonic generation microscopic planar view of the stroma on-chip showing an extensive network of long collagen fibers in the Cervix Chip (collagen, turquoise) (middle bottom) (bar, 50 µm). Pseudo-H&E cross section views of the Cervix Chips developed using periodic (top right) and continuous (bottom right) flow conditions. (bar, 20µm). **c.** Immunofluorescence microscopic views of cervical epithelium stained for F-actin (yellow) and viewed from above (bar 50 µm) (left) and graphs showing mucus levels (top right) and

transepithelial electrical resistance (TEER) (bottom right) in Transwell cervical epithelial cell cultures with (+) and without (-) stromal cells. **d.** Quantification of the change in the epithelial cells growth and differentiation in Cervix Chip measured by left) percentage change in the number of cells stained for Ki67, and right) surface area (μm^2) stained for MUC5B per cell in the epithelium throughout the culture time. Data represents the mean \pm s.e.m.; n=3 (**c**), and 3 (**d**) experimental chip or Transwell replicates. Source data and statistical tests are provided as a Source Data file. Micrographs are representatives of three separate experiments.

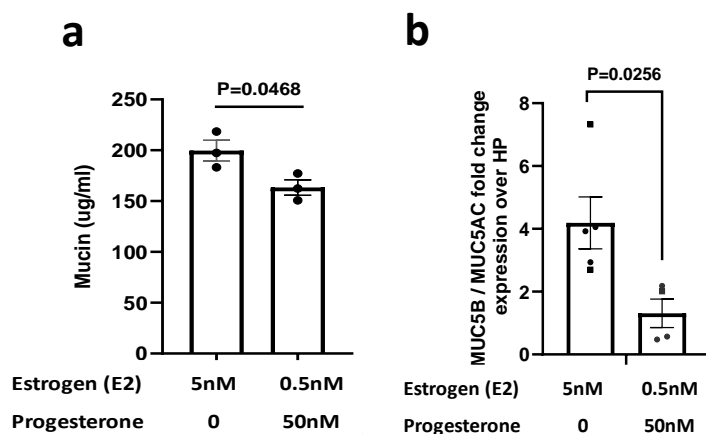


Supplementary Fig. S2. Cervix Chip comparison with static cultures. **a.** Graph showing fold change in expression of cervical epithelial genes encoding mucin 4 (*MUC4*), mucin 5B (*MUC5B*), and secretory leukocyte peptidase inhibition (*SLPI*) in periodic flow Cervix Chip and Transwell compared to 2D culture. **b.** Graph showing real-time changes in the Cervix Chip transepithelial electrical resistance TEER measured using custom made Organ Chip with integrated electrodes compared to Transwell culture measured using IVUM2 (red arrow indicates start of differentiation in culture). **c.** Gene set scoring

analysis showing relative ratio of the upregulated epithelial genes relative to the signature ectocervical genes in Cervix Chip cell developed using periodic and continuous flow regimen and Transwell culture for three different donors quantified using bulk RNAseq analysis of cervical epithelial cells. **d.** Left) Phase-contrast and (middle) immunofluorescence microscopic view of cervical epithelium in a Transwell (TW, top) and Cervix Chip (bottom) culture, and right) immunofluorescence microscopic view of fibroblast stroma stained for F-actin (yellow) (bar 50 μ m). **e.** Gene set scoring analysis showing the relative ratio of the top 50% highly expressed collagens in GTEx tissue samples (*COL1A1*, *COL1A2*, *COL3A1*, *COL4A1*, *COL4A2*, *COL4A4*, *COL4A5*, *COL4A6*, *COL5A1*, *COL5A2*, *COL5A3*, *COL6A1*, *COL6A2*, *COL6A3*, *COL7A1*, *COL8A1*, *COL9A2*, *COL11A2*, *COL12A1*, *COL13A1*, *COL14A1*, *COL15A1*, *COL16A1*, *COL17A1*, *COL18A1*, *COL21A1*, *COL22A1*, *COL23A1*, *COL24A1*, *COL27A1*) in cervical epithelial cells of Cervix Chips developed using periodic and continuous flow regimen, and Transwell culture for three different donors, and 10 endocervical and 9 ectocervical tissue samples from GTEx quantified using bulk RNAseq analysis. Data represents the mean \pm s.e.m.; n=3 (**a**), 8 (**b**), 3 (**c**), and 3 (**e**) experimental chip or Transwell replicates. Micrographs in (**d**) are representatives of three separate experiments. Source data and statistical tests are provided as a Source Data file.



Supplementary Fig. S3. Cervix Chip responses to changes in pH. **a.** Graph showing changes in the pH of the Cervix Chip inflow and outflow media when cultured at pH 7.1 compared to pH 5.4. **b.** Quantification of permeability in Cervix Chip cultured under at pH 7.1 compared to pH 5.4 as measured by apparent permeability (P_{app}). **c.** Quantification of total mucin content produced by each cell in Cervix Chip cultured at pH 7.1 compared to pH 5.4 using an Alcian Blue assay. **d.** Graph showing fold change in the expression of cervical epithelial genes encoding mucin 5B (*MUC5B*) and asparaginase and isoaspartyl peptidase (*ASRGL*) in Cervix Chip cultured at pH 7.1 and pH 5.4 using real-time PCR. Data represent the mean \pm s.e.m.; $n=4$ (**a**), 5 (**b**), 3 (**c**), and 5 (**d**) experimental chip replicates; *n.s.*, not significant Source data and statistical tests are provided as a Source Data file.

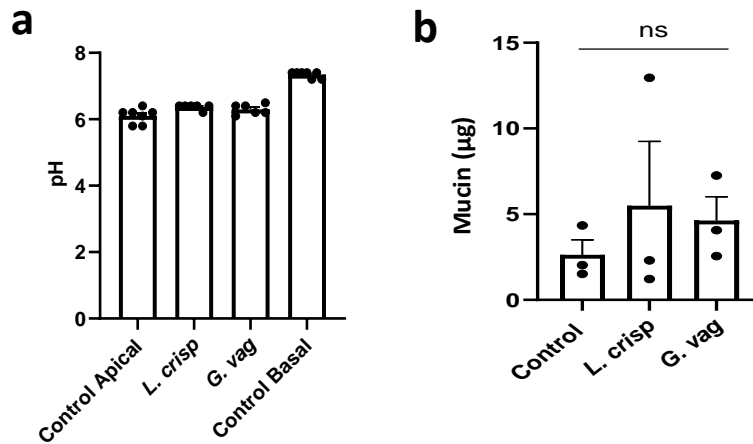


c

Class (Compound Retention time)	Human Clinical Mucus	Cervix Chip HE	Cervix Chip HP
O-glycans			
Sialylated (2_2_0_2 28.2)	x	x	↓
Fucosylated (2_2_1_0 18.9)	x		
Sialylated and fucosylated (2_2_1_1 27.0)	x		
Sialylated (2_2_0_1 19.3)	x	x	↑
Sialylated and fucosylated (1_1_1_1 25.8)	x		
Fucosylated (2_2_2_0 21.9)	x		
Sialylated (3_3_0_1 21.6)	x		
Sialylated and fucosylated (2_2_1_2 24.7)	x	x	↓
Sialylated (3_3_0_2 24.8)	x	x	
Sialylated (2_2_0_2 26.1)	x		x
N-glycans			
Sialylated (6_5_0_3 30.9)	x	x	↓
Sialylated (5_4_0_2 25.9)	x	x	↓
Sialylated (5_4_0_2 25.1)	x	x	↓
Sialylated and fucosylated (5_4_1_2 26.7)	x	x	↓
Sialylated (5_4_0_1 24.0)	x	x	↓
Sialylated and fucosylated (6_5_1_3 29.3)	x		
Sialylated (7_6_0_3 31.5)	x		
Sialylated (5_4_0_2 27.5)	x	x	↓
Sialylated (6_5_0_2 26.6)	x		
Sialylated and fucosylated (5_4_1_1 25.3)	x	x	x
Sialylated (5_4_0_1 23.1)	x	x	↓
Fucosylated (5_4_1_0 22.6)	x	x	↓

Supplementary Fig. S4. Cervix Chip responses to sex hormones. **a.** Quantification of total mucin content produced by Cervix Chip cultured with high estrogen (5nM E2+0nM P4) compared to high progesterone (0.5nM E2+50nM P4) hormone levels using Alcian Blue assay. **b.** Graph showing change in expression level ratio of cervical genes encoding mucin 5B (*MUC5B*) and mucin 5AC (*MUC5AC*) in the Cervix Chips culture with high estrogen (5nM E2+0nM P4) compared to high progesterone (HP, 0.5nM E2+50nM P4) hormone levels. **c.** Changes in the abundance of O- and N-glycan compounds in the mucus collected from Cervix Chip cultured with high estrogen (HE, 5nM E2+0nM P4) compared to high progesterone (HP,

0.5nM E2+50nM P4) levels detected using nanoLC-QTOF MS/MS glycomic analysis (upward and downward arrows indicate increase and decrease, respectively, in the relative abundance of glycans in the HP compared to HE chips). Data represent the mean \pm s.e.m.; n=3 (**a**), and 5 (**b**) experimental chip replicates. Source data and statistical tests are provided as a Source Data file.



Supplementary Fig. S5. Cervix Chip responses to bacteria. **a.** Graph showing changes in the pH of the Cervix Chip epithelium effluents co-cultured in the absence or presence of *L. crispatus* or *G. vaginalis* consortia at 72 hours post inoculation compared to control basal channel. **b.** Quantification of total mucin content in the Cervix Chip effluents co-cultured with *L. crispatus* or *G. vaginalis* consortia compared to control chip without bacteria using an Alcian Blue assay. Data represent the mean \pm s.e.m.; $n=7$ (**a**), and 3 (**b**) experimental chip replicates; n.s., not significant. Source data and statistical tests are provided as a Source Data file.